Removal of a cationic dye from wastewater by adsorption onto natural adsorbents

H. Ouasif [1*], S. Yousfi [1], M.L. Bouamrani [1], M. El Kouali [1], S. Benmokhtar [2], M. Talbi [1]

[1]*Laboratoire de Chimie Analytique Physico-Chimie des Matériaux, Département de Chimie, Faculté des Sciences Ben M'Sik Casablanca, Maroc.*
[2]*Laboratoire de Recherche de Chimie-Physique Générale des Matériaux, Département de Chimie, Faculté des Sciences Ben M'Sik Casablanca, Maroc.*

Abstract
The aim of this study is the elimination of methylene blue from waste water by adsorption on clays and oil shales. These natural materials are decarbonated with hydrochloric acid and characterized by X-ray diffraction, X-ray fluorescence and infrared spectroscopy. Factors affecting adsorption were evaluated. Kinetic parameters calculated from the experimental data could be fitted to a pseudo-second-order kinetic model. The equilibrium of adsorption and the adsorption data are well described by the Langmuir model. Clays absorb more methylene blue than oil shales. The sorbents treated with hydrochloric acid have higher capacity than the starting materials.

Keywords: Clay, Oil shales, Adsorption, Methylene blue, Kinetics, Isotherms.

1. Introduction
Organic dyes released to surface waters during printing and dyeing of textiles and clothing may be toxic above certain threshold concentrations to aquatic organisms [1; 2]. In addition, dye-containing wastewaters are commonly characterized by high salt content and slow biodegradation [3] which makes removal by conventional wastewater treatment processes difficult [4].

One of the most effective methods for removal of organic dye pollutant is by adsorption [5; 6]. The capacity depends on the physical nature of adsorbent, the nature of adsorbate, and the condition solutions [7]. Activated carbon is a frequently used method to prevent toxic pollutants from entering the water environment [8] but is an expensive material its use for pollution control applications cannot be justified [9]. The research has been directed towards methods of treatment using natural materials, locally available and effective adsorbents, such as waste biopolymers [8; 10], clays and clay minerals [4; 11; 12], industry waste [13], agricultural waste [14; 15].

Clays are sedimentary rocks which constitute a major component of the earth's crust. In fact more or less hydrated aluminosilicates have a structure of very great specific surface associated very particular physicochemical characteristics.

Oil shales are present in the form of a mixture of two matters [16]; an organic matter which originates in the matter presents initially in the plants and the micro-organisms, and a mineral matter which comes from the minerals which constitute vegetable fabrics and minerals deposited by sedimentation.

The natural samples were decarbonated by hydrochloric acid and each type of adsorbent was characterized, by X-ray powder diffraction, X-ray fluorescence and Fourier transform infrared spectroscopy, before its use of methylene blue adsorption. In this part; laboratory batch isotherm studies were conducted to evaluate the adsorption capacity of adsorbents. The effects of initial dye concentration, weight, granulometry, contact time and temperature were also investigated. Langmuir and Freundlich isotherm models were tested for their applicability with the experimental data.

2. Materials and methods

2.1. Preparation and characterization of adsorbents

In this study we used two types of samples: clays and oil shales natural and decarbonated.

In the first time, the samples were prepared in the following conditions: Rocks were crushed and powdered. Fractions of the product were attacked by the hydrochloric acid HCl (6N) [17]. This attack is conducted until the disappearance of the CO_2 release. After filtration, the residues obtained are washed by distilled water to eliminate excess acid. Then, the samples are dried then dried in steam at 80 °C during 12 h, crushed and sieved by a series of AFNOR sieves, the powder used for the experiments having a granulation between 0.63 and 0.1 mm.

Natural clays abbreviated NC, natural oil schales abbreviated NOS, decarbonated clays abbreviated DC and decarbonated oil schales abbreviated DOS materials have been studied by several methods. The chemical compositions of the samples were estimated by X-ray fluorescence (XRF, Axios; PANalytical). X-Ray Diffraction spectroscopy (XRD) analysis was carried out with Philips X'Pert PRO CuKα. A dried sample of the produced material was ground using an agate mortar and pestle and tested at 40 kV and 40 mA. Fourier transform infrared spectrophotometry (FTIR, VERTEX 70) analysis was conducted for the produced samples by mixing a pre-dried sample of 3 mg with blank KBr and pressed hydraulically at 10 tons m^{-2} to obtain a thin transparent disk, then analyzed using VERTEX 70 spectrophotometer.

2.2. Preparation and characterization of adsorbate solutions

All chemicals used in this study were of Merck-grade. Methylene Blue (MB), the basic dye used as the model sorbate in the present study is a monovalent cationic dye. It is classified as CI Basic blue 9, CI solvent blue 8, CI 52015. It has a molecular formula $C_{16}H_{18}N_3ClS$ and molecular weight of 319.85. The MB was chosen in this study because of its known strong adsorption onto solids.

The MB used was of Merck grade so it was used without further purification. A stock solution of 1 g/L was prepared by dissolving an appropriate quantity of MB in a liter of distilled water. The working solutions were prepared by diluting the stock solution with distilled water to give the appropriate concentration of the working solutions.

2.3. Analysis

The concentration of the residual dye was measured using UV/visible spectrometer at a λ_{max} corresponding to the maximum absorption for the dye solution (λ_{max}=664 nm) by withdrawing samples at fixed time intervals, centrifuged and the supernatant was analyzed for residual MB.

2.4 Adsorption experiments

All sorption experiments were agitated in a batch reactor at atmospheric pressure, without adjusting the pH, at room temperature and the shaking rate was the same for all the experiments.

2.4.1. The effects of various parameters influencing the adsorption

In order to evaluate the effect of parameters influencing the adsorption of MB, we studied the effect of a series of factors (quantity and granulometry of adsorbents, initial adsorbate concentration and temperature) likely to intervene in the process of this phenomenon.

2.4.2. Adsorption Kinetics

About 0.4 g of the samples was introduced into a 400 mL of MB solution of 50 mg/L and kept in a laboratory shaker for various mixing time. Filter-separating of solid phase from liquid was followed by centrifuging at 3000 rpm for 10 min. The MB solutions were diluted using distilled water and MB residual concentration was determined as mentioned above.

2.4.3. Adsorption isotherms

Adsorption isotherms are important for the description of how adsorbates will interact with an adsorbent and are critical in optimizing the use of adsorbent [18]. Thus, the correlation of equilibrium data using either a theoretical or empirical equation is essential for adsorption data interpretation and prediction. Several mathematical models can be used to describe experimental data of adsorption isotherms. Two famous isotherm

equations, the Langmuir, and Freundlich, were employed for further interpretation of the obtained adsorption data.

3. Results and discussion

3.1. Samples characterization

The X-ray diffractogram (Fig.1) of the powder produced from the natural samples (NOS and NC), shows that it is composed essentially of carbonates (calcite and dolomite) and silicates. Moreover, we also note the presence, in the X-ray diffractogram of NC and DC, of the characteristic peaks of Illite and kaolin. The analyses of the DC and DOS samples, resulting from the treatments of NC and NOS respectively, shows the absence of the major carbonate peaks, which confirms the major elimination of this constituent by the HCl treatment. Under these conditions, the peaks relative to SiO_2 become stranger.
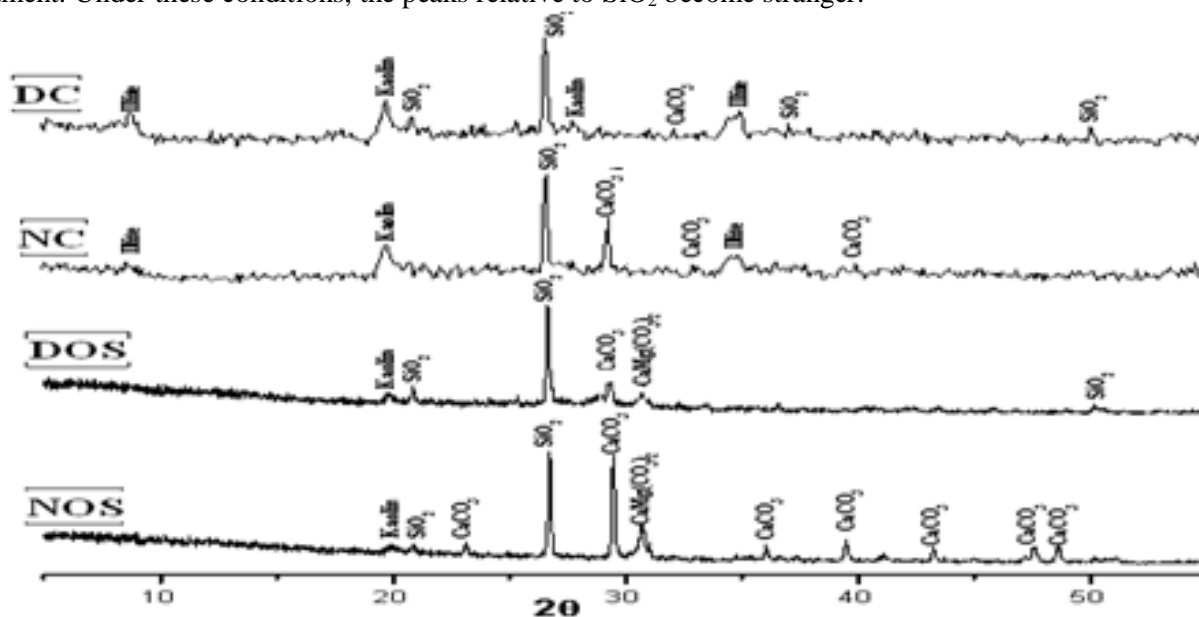

Figure 1. X-ray diffraction patterns of various samples

The composition confirmed by X-ray fluorescence data (Table 1) showing the presence of SiO_2, CaO, Al_2O_3, MgO and Fe_2O_3 as major elements in NC and NOS. The elemental chemical analysis of decarbonated samples shows that it is enriched in SiO_2, Al_2O_3, and Fe_2O_3, On the other hand, the contents of CaO and MgO knew a significant decreased.

Table 1: Chemical compositionsof various samples by X-ray fluorescence (mass %)

Samples	SiO_2	Al_2O_3	Fe_2O_3	CaO	MgO	K_2O	P_2O_5	Na_2O	TiO_2	SO_3	LOI (Loss on ignition)	Total
NC	42,62	15,76	4,96	10,48	4,39	2,93	2,96	0,57	0,65	0,26	14,23	99,81
DC	53,25	22,19	7,73	2,85	1,72	1,86	1,44	0,33	0,94	0,11	7,15	99,57
NOS	21,81	5,76	2,3	21,71	3,28	0,73	0,92	0,17	0,2	3,31	39,70	99,89
DOS	35,94	7,63	3,17	16,77	1,64	1,25	1,05	*	0,39	4,25	27,63	99,72

The FTIR spectrum (Fig.2) of the NOS and NC displays characteristic carbonate absorption bands (1429, 875 and 712 cm^{-1}) and silicates (1035 cm^{-1}). We also note the presence of the characteristic bands of several chemical functions (aliphatic, unsaturated, aromatic, carboxylic, etc.) in the FTIR spectrum of NOS.

The analyses of the DC and DOS samples, shows the absence of the major carbonate peaks and the peaks relative to SiO_2 become stranger.
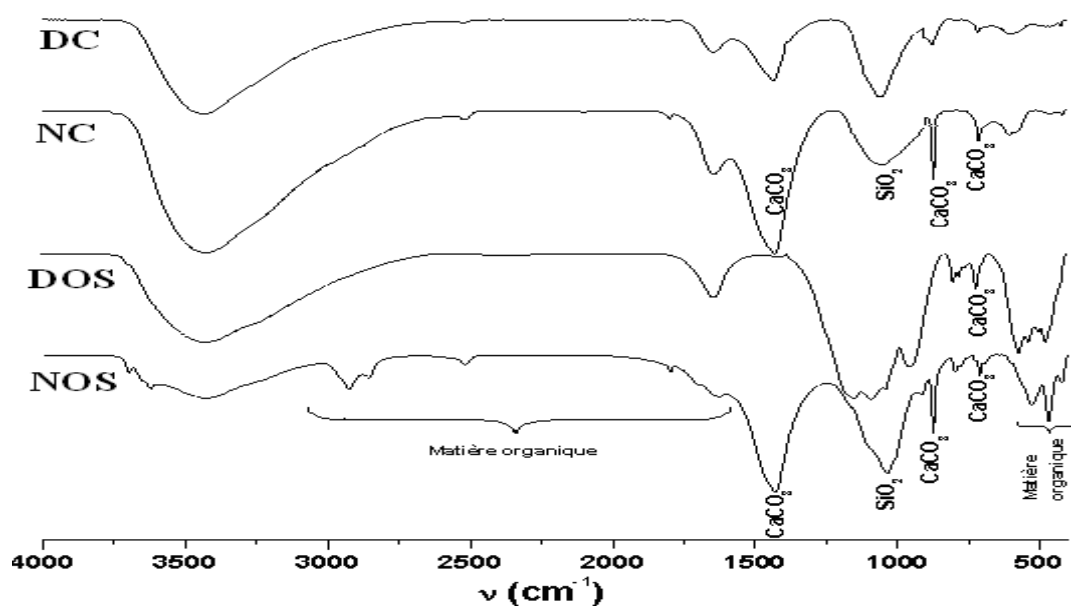
Figure 2. FT-IR spectrum of various samples

3.2. Adsorption experiments
3.2.1. Influence of some parameters on adsorption
The effects of various parameters such as quantity (Fig.3) and granulometry (Fig.4) of adsorbents, initial MB concentration (Fig.5) and temperature (Fig.6) were investigated.

3.2.1.1. Effect of quantity on the adsorption MB
Fig.3 represents the effect of weight of adsorbents on the adsorption of MB by various adsorbents. It was found that the adsorption increases with an increase in the weight; this is because the adsorption depends on the external surface of the adsorbent material increases with a large mass.
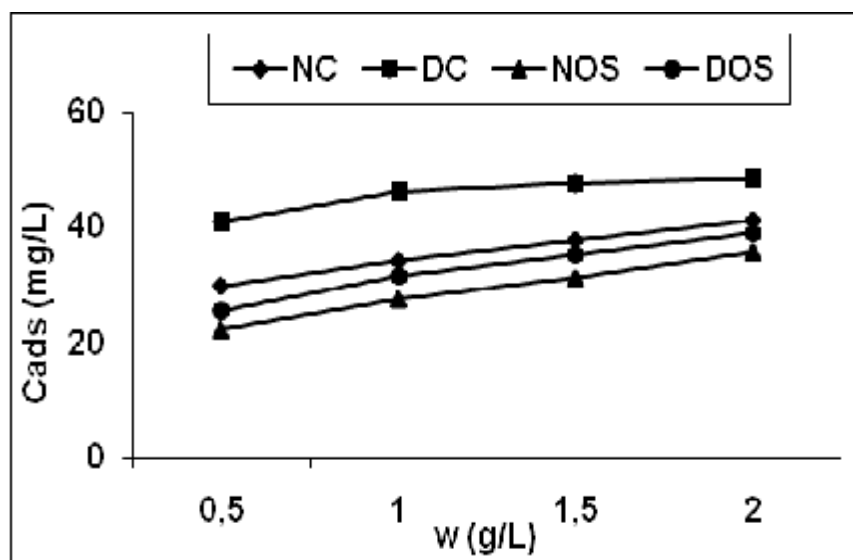

Figure 3. Effect of quantity of adsorbents

3.2.1.2. Effect of granulometry on the adsorption MB
The effect of granulometry on the dye adsorption listed in Fig.4. The data indicate that the adsorption capacity increased as a particle size of adsorbent decreased. This is because the adsorption depends on the external surface of the adsorbent material increases with the fineness of its particles.
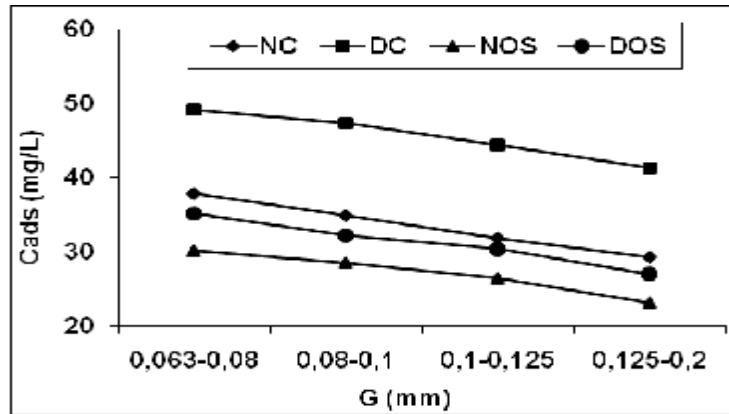
Figure 4. Effect of Granulometry of adsorbents

3.2.1.3. Effect of initial MB concentration on the adsorption

The effect of the initial MB concentration, on the adsorption capacity, is shown in Fig.5. The amount of MB adsorbed increased with the increase in the concentration MB. This means, when the initial concentration increased from 25 to 125 mg/L. It was because the initial concentration plays an important role which provided the necessary driving force to overcome the resistances to the mass transfer of MB between the aqueous and the solid phases [19]. The interaction between adsorbate and adsorbent was also found to enhance with the increase in the initial concentration. Thus, it can be concluded that higher initial concentration enhances the adsorption uptake of MB.
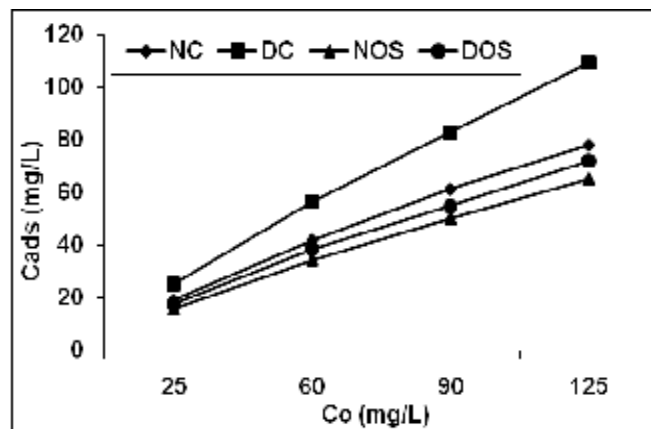

Figure 5. Effect of initial MB concentration

3.2.1.4. Effect of temperature on the adsorption of MB

To observe the effect of temperature on the adsorption of MB by the various adsorbents, experiments are carried at three different temperatures (30, 40, 50 and 60 °C). It has been observed that with increase in temperature, adsorption capacity increases as shown in Fig.6. This setting will affect this process positively by high energy contribution, as it allows overcoming the repulsive forces localized at the interfaces of liquids and solids. Therefore, the contribution of heating plays an important role in the retention of this dye.

3.2.2. Kinetics studies

The effect of the contact time on the adsorption capacity of adsorbents is shown in Fig.7. The contact time varied in the range 0-420 min. As Fig.7 shows, the time required to achieve the equilibrium was about 100 min. One can see that the adsorption is rapid in the first minutes of contact time. The nature of the samples had a marked effect in MB removal, leading to the clays having higher adsorption capacity than the oil shales. The higher amount of MB adsorption, Qe, number implied a higher selectivity or adsorption for decarbonated samples more than natural samples. The selectivity of the four adsorbents based on Qe values followed the order:
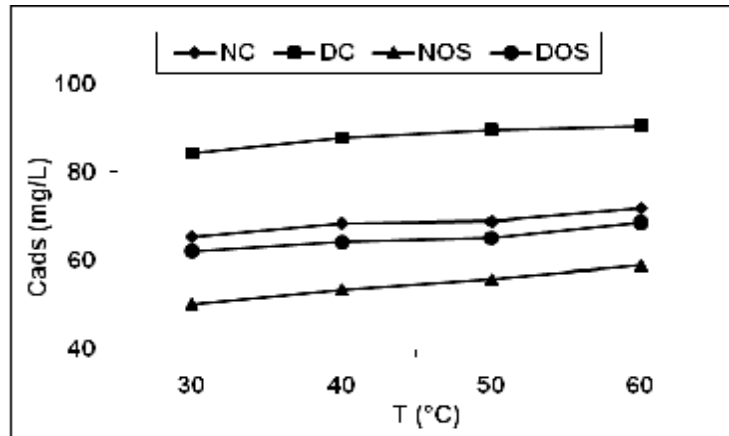
NOS < DOS < NC < DC
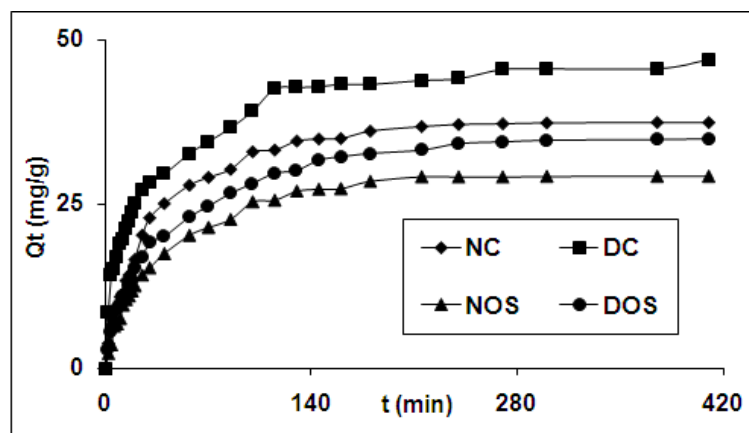
Figure 6. Effect of Temperature

Figure 7. Adsorption kinetics of MB

It is important to be able to predict the rate at which contamination is removed from aqueous solutions in order to design an adsorption treatment plant. In order to investigate the mechanism of adsorption and potential rate controlling steps such as mass transfer and chemical reaction, the kinetics of MB sorption onto clays and oil shales was investigated using two different models: the pseudo-first-order [20; 21], and the pseudo second-order [22; 23] kinetic models. The conformity between experimental data and the model predicted values was expressed by the correlation coefficients (R^2, values close or equal to 1). A relatively high R^2 value indicates that the model successfully describes the kinetics of MB adsorption.

The pseudo-first order equation (Eq. (1)) is one of the most widely used equation, being the first rate equation developed for sorption in solid/liquid systems:

$$\ln(q_e - q_t) = \ln(q_e) - k_{1app}.t \tag{1}$$

Where: Qe and Qt are the adsorption capacity at equilibrium and at time t, respectively (mg/g), k_1 is the rate constant of pseudo first-order adsorption (L/min),

The slopes and intercepts of the plots [log(Qe−Qt)] vs t (Fig.8) were used to determine the pseudo-first order rate constant, k_1, and Qe, the values obtained being presented in Table 2.

The theoretical (Qe,cal) values estimated from the pseudo-first order kinetic model gave significantly different values compared to experimental (Qe,exp) values (Table 2). These results showed that the pseudo-first-order kinetic model did not describe well these adsorption systems.

The adsorption data were also treated according to the pseudo-second order kinetics using the (Eq. (2)):

$$\left(\frac{t}{q_t}\right) = \left(\frac{t}{q_e}\right) + \left[\frac{1}{k_{2app.}(q_e)^2}\right] \tag{2}$$

Where: k_2 is the rate constant of pseudo-second-order (g mg^{-1} min^{-1}).

The values of k_2 and Qe were obtained from the intercept and slope of the straight lines resulted by plotting t/Q$_t$ against t (Fig.9) and were presented in Table 2.
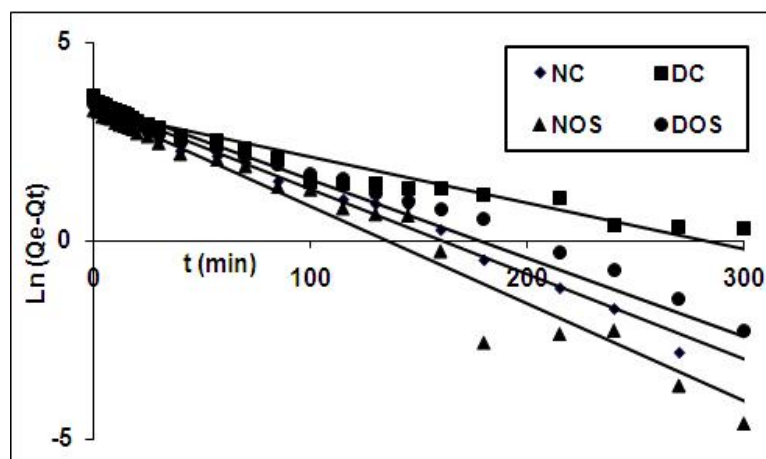
J. Mater. Environ. Sci. 4 (1) (2013) 1-10
Ouasif et al.

ISSN : 2028-2508
CODEN: JMESCN

Figure 8. The applicability of the pseudo-first-order kinetic model

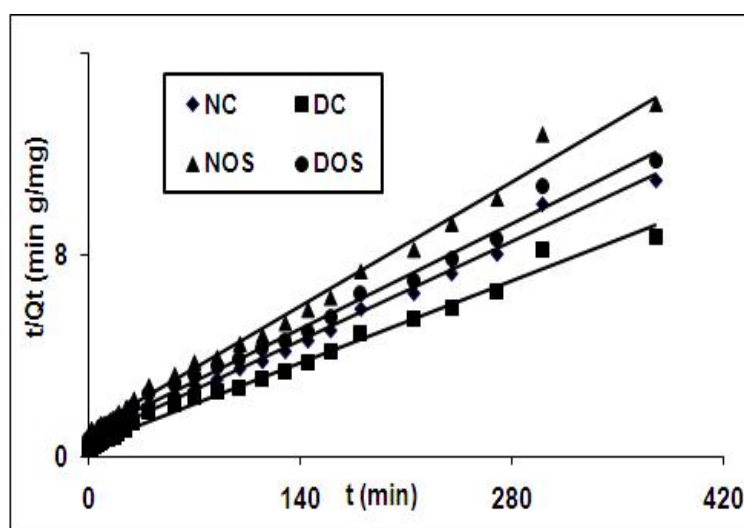**Figure 9.** The applicability of the pseudo-second-order kinetic model

As Table 2 shows, the theoretical (Qe,cal) values, estimated from the pseudo-second order kinetic model, are very close to the experimental (Qe,exp) values (Table 2). Furthermore, all the correlation coefficients R^2 values are close to 1 confirming the applicability of the pseudo-second-order equation. Several studies [24-26] found that the kinetics of adsorption of dyes on clay materials obey the pseudo-second-order.

Table 2: Kinetic parameters for MB adsorption

Adsorbents	$Q_{e.exp}$ (mg g^{-1})	pseudo-first-order			pseudo-second-order		
		$Q_{e.cal}$ (mg g^{-1})	k_1 (min^{-1})	R^2	$Q_{e.cal}$ (mg g^{-1})	k_2 (g min^{-1} mg^{-1})	R^2
NC	37.27	30.53	2.14 10^{-2}	0.978	35.46	1.17 10^{-3}	0.994
DC	46.97	26.34	1.16 10^{-2}	0.944	42.55	1.27 10^{-3}	0.991
NOS	29.22	27.57	2.45 10^{-2}	0.974	28.25	1.28 10^{-3}	0.993
DOS	34.93	33.08	1.98 10^{-2}	0.958	33.44	1.04 10^{-3}	0.993

3.2.3. Adsorption isotherms

The adsorption isotherms were determined by shaking 1 g/L of the adsorbents with 100 mL of 20 to 160 mg/L of MB solutions for 16 h.

The adsorption isotherms of MB for all systems used were obtained in an attempt to get a more thorough insight to the adsorption mechanism of MB onto the clays and the oil shales. The isotherms for all systems

were given in Fig.10. They were classified as the L curves of Giles' classification [27; 26], in which the solution has such a high affinity for the solute that in dilute solutions it is, completely, adsorbed resulting in a vertical initial part of the isotherm.
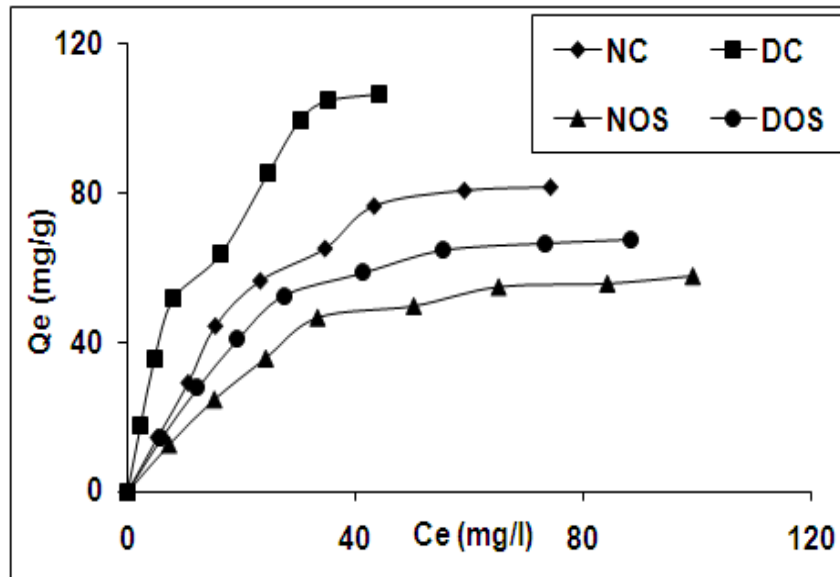

Figure 10. Adsorption isotherms for MB adsorption

The experimental data of MB adsorption (Fig.10) were regressively analyzed with the Freundlich and Langmuir models.

The Freundlich isotherm [29] is the earliest known relationship describing the adsorption. The equation is conveniently used in the linear form as:

$$\log q_e = \log K_F + n \log C_e \tag{3}$$

Where K_F (mg^{1-n} g^{-1} L^n) is the adsorption capacity and 'n' is the Empirical parameter representing the energetic heterogeneity of the adsorption sites. A plot of (Ln Qe) against (Ln Ce) yields a straight line which indicates the confirmation of the Freundlich isotherm for adsorption. The constants (K_F and n) can be obtained from the slope and the intercept of the linear plot of the experimental data.

The Langmuir adsorption isotherm [30] is often used for adsorption of the solute from a liquid solution, the above equation can be used to create the following linear form [31]:

$$\frac{1}{q_e} = \frac{1}{C_e} \frac{1}{K_L q_m}) + \frac{1}{q_m} \tag{4}$$

where Qm (mg/g) is the maximum adsorption capacity corresponding to complete monolayer coverage and K_L (L/mg) is the Langmuir constant relating to adsorption energy. The linear form can be used for the linearization of experimental data by plotting Ce/Qe against Ce.

The essential characteristics of the Langmuir equation can be expressed in terms of dimensionless separation factor, R_L, defined as [33]:

$$R_L = \frac{1}{1 + K_L.C_0} \tag{5}$$

Where, C_o (mg/L) is the adsorbate initial concentration.
The R_L value implies the adsorption to be defavourable ($R_L > 1$), linear ($R_L = 1$), favourable ($0 < R_L < 1$), or irreversible ($R_L = 0$).
The linearized Freundlich and Langmuir plots were given in Fig. 11 and Fig. 12, respectively and the constants K_F, n, Q_m, K_L, R_L (Moyenne value) and R^2 (for each model) are tabulated in Table 3.
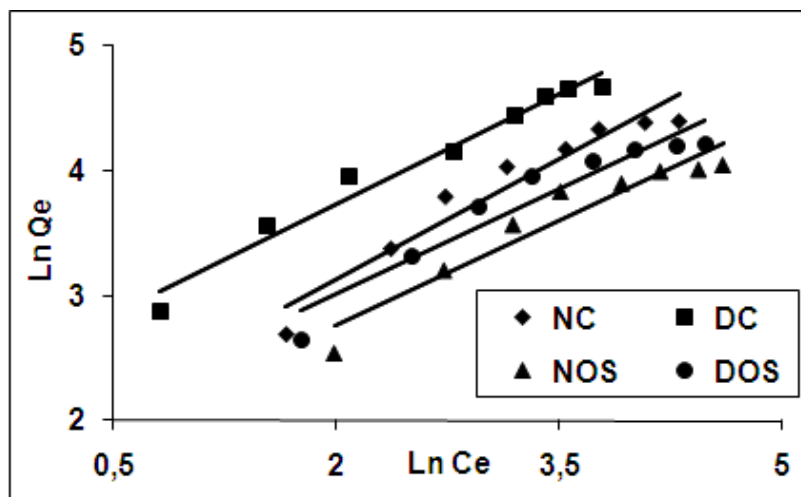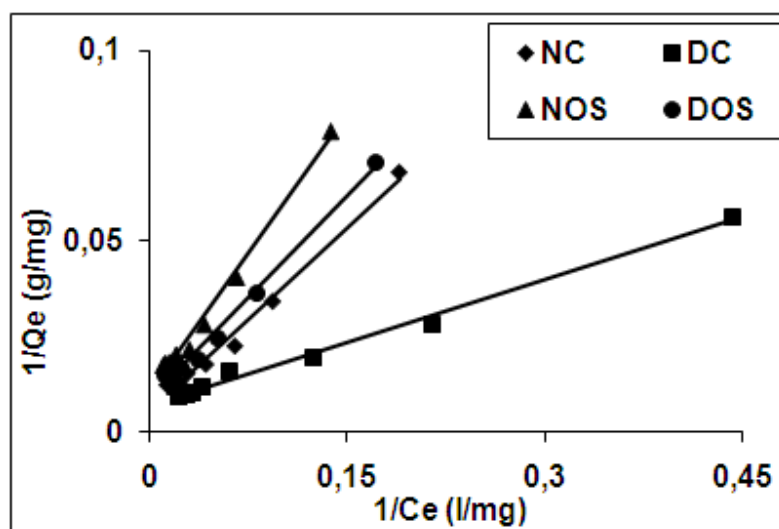
Figure 11. Freundlich isotherm models

Figure 12. Langmuir isotherm models

From Table 3, the correlation coefficients values ($R^2 > 0.99$ for Langmuir model) indicate that the adsorption of MB onto clays and oil schales follows the Langmuir model better than the Freundlich model; this shows that the isotherm data type L are best described by the Langmuir model [32].

Comparison of the oil schales adsorption capacity and the clays adsorption capacity indicated that the clays had a higher selectivity for MB removal. Additionally, the decarbonated adsorbents removed higher quantities of MB more than the similar natural adsorbents.

The R_L values are between 0 and 1 in all the experimental systems, which confirm the favourable uptake of the MB process.

Table 3: Isotherm parameters

Adsorbents	Freundlich parameters			Langmuir parameters			
	K_F $(mg^{1-n}\ g^{-1}\ L^n)$	n	R^2	Q_m $(mg\ g^{-1})$	K_L $(L\ mg^{-1})$	R_L	R^2
NC	6.34	0.64	0.931	140.84	0.022	0.38	0.989
DC	12.94	0.59	0.927	188.68	0.049	0.23	0.991
NOS	5.47	0.56	0.915	99.01	0.021	0.39	0.990
DOS	6.57	0.57	0.916	117.65	0.025	0.36	0.991

Conclusion

In the light of the finding of this work, the following main conclusions can be stressed:

(1) The analysis of decarbonated materials by X-ray diffraction, X-ray fluorescence and Fourier transform infrared spectroscopy revealed that the levels of SiO_2 and Al_2O_3 have experienced a significant increase. In contrast, CaO and MgO contents decreased.

(2) The amount of dye removed increased with increasing weight, initial dye concentration and temperature and decreased with increase in granulometry.

(3) The adsorption behaviour of MB onto the composite adsorbent was investigated. It was found that clays composite adsorbent is effective sorbent for MB and the decarbonated clays adsorbent exhibited excellent adsorption selectivity for MB.

(4) The adsorption kinetic process was described by a pseudo-second-order rate model very well.

(5) The isotherm study indicates that adsorption data can be adequately modelled by the Langmuir.

References

1. Al-Degs, Y., Khraishen, M., Allen, S.J., Ahmad, M.N., *Water. Res*. 34 (2000) 927.
2. Ozkaya, B., *J. Hazard. Mater*. B129 (2006) 158
3. Alinsafi, A., Khemis, M., Pons, M.N., Leclerc, J.P., Yaacoubi, A., Benhammou, A., Nejmeddine, A., *Chemical Engineering & Processing*. 44 (2005) 461
4. Vimonses, V., Lei, S., Jin, B., Chow, C.W.K., Saint, C., *Applied Clay Science*. 43 (2009) 465
5. Crini, G., Badot, P.M., *Progress in Polymer Science*. 33 (2008) 399
6. Basar, C. A., *J. Hazard. Mater.* 135 (2006) 232
7. Wang, S., Zhu, Z.H., *Dyes and Pigments*. 75 (2007) 306
8. Hsieh, C.T., Teng, H., *Carbon*. 38 (2000) 863
9. Attia, A.A., Girgis B.S., Fathy, N.A., *Dyes and Pigments*. 76 (2008) 282
10. Cheung, W.H., Szeto Y.S., McKay, G., *Bioresource Technology*. 100 (2009) 1143
11. Gecol, H., Miakatsindila, P., Ergican, E., Hiibel, S.R., *Desalination*. 197 (2006) 165
12. Karim, A.B., Mounir, B., Hachkar, M., Baasse, M., Yaacoubi, A., *J. Hazard. Mater*. 168 (2009) 304
13. Mittal, A., Mittal, J., Malviya, A., Kaur D., Gupta, V.K., *J. Colloid. Interf. Sci*. 343 (2010) 463
14. Uddin, M.T., Islam, M.A., Mahmud, S., Rukanuzzaman, M., *J. Hazard. Mater*. 164 (2009) 53
15. Zhenhu, H., Hui, C., Feng J., Shoujun, Y., *J. Hazard. Mater*. 173 (2010) 292
16. Bekri, O., Ziyad, M., Abstract presented at Oil Shale Symposium, Lexington, Kentucky, U.S.A, (1991).
17. Moore, S.W., Reid, F.D., *J. Geophysical Research*. 78 (1973) 8880
18. Roostaei, N., Tezel, F.H., J. *Environmental Management*. 70 (2004)157
19. Srivastava, V.C., Swamy, M.M., Mall, I.D., Prasad, B., Mishra, I.M., *Colloids and Surfaces*. 272 (2006) 89
20. Lagergren, S., *Handlingar*. 24 (1898) 1
21. Ho, Y.S., McKay, G., *Process Safety and Environmental Protection*, 76B (1998) 313
22. Ho, Y.S., McKay, G., *Water. Res.* 34 (2000) 735
23. Kumar, K.V., *J. Hazard. Mater*. 142 (2007) 564
24. Yener, J., Kopac, T., Dogu, G., *Journal of Colloid and Interface Science*. 294 (2006) 255
25. Janos, P., Michalek, P., Turek, P., *Dyes and Pigments*. 74 (2007) 363
26. Wang, S., Li, H., *J. Hazard. Mater*. B126 (2005) 71
27. Giles, C.H., Smith, D., Huitson, A., *Journal of Colloid and Interface Science* 47 (1974) 755
28. Limousin, G., Gaudet, J.P., Charlet, L., Szenknect, S., Barthes, V., Krimissa, M., *Applied Geochemistry*. 22 (2007) 249
29. Freundlich, H., *J. Z Phys. Chem.* 57 (1906) 385
30. Langmuir, I., *J. Am. Chem. Soc.* 40 (1918) 1361
31. Hamdaoui, O., Naffrechoux, E., *J. Hazard. Mater*. 147 (2007) 381
32. Hinz, C., *Geoderma*. 99 (2001) 225
33. Hall, K.R., Eagleton, L.C., Acrivos, A., Vermeulen, T., *Industrial and Engineering Chemistry Fundamentals*. 5 (1966) 212